

# TCB2, a new anti-human interleukin-2 antibody, facilitates heterodimeric IL-2 receptor signaling and improves anti-tumor immunity

Jun-Young Lee, Eunjin Lee, Sung Wook Hong, Daeun Kim, O. Eunju, Jonathan Sprent, Sin-Hyeog Im, You Jeong Lee & Charles D. Surh

To cite this article: Jun-Young Lee, Eunjin Lee, Sung Wook Hong, Daeun Kim, O. Eunju, Jonathan Sprent, Sin-Hyeog Im, You Jeong Lee & Charles D. Surh (2019): TCB2, a new anti-human interleukin-2 antibody, facilitates heterodimeric IL-2 receptor signaling and improves anti-tumor immunity, *Oncoimmunology*, DOI: [10.1080/2162402X.2019.1681869](https://doi.org/10.1080/2162402X.2019.1681869)

To link to this article: <https://doi.org/10.1080/2162402X.2019.1681869>



© 2019 The Author(s). Published with license by Taylor & Francis Group, LLC.



View supplementary material [↗](#)



Published online: 04 Nov 2019.



Submit your article to this journal [↗](#)




View related articles [↗](#)



View Crossmark data [↗](#)

## TCB2, a new anti-human interleukin-2 antibody, facilitates heterodimeric IL-2 receptor signaling and improves anti-tumor immunity

Jun-Young Lee<sup>a,b,#</sup>, Eunjin Lee<sup>b</sup>, Sung Wook Hong<sup>a\*</sup>, Daeun Kim<sup>a,b</sup>, O. Eunju<sup>a,b</sup>, Jonathan Sprent<sup>d,e</sup>, Sin-Hyeog Im<sup>a,b</sup>, You Jeong Lee <sup>a,b</sup>, and Charles D. Surh<sup>a,b,c†</sup>

<sup>a</sup>Academy of Immunology and Microbiology, Institute for Basic Science (IBS), Pohang, Republic of Korea; <sup>b</sup>Division of Integrative Biosciences & Biotechnology, Pohang University of Science and Technology (POSTECH), Pohang, Republic of Korea; <sup>c</sup>Division of Developmental Immunology, La Jolla Institute for Allergy and Immunology, La Jolla, CA, USA; <sup>d</sup>Department of Immunology, Garvan Institute of Medical Research, Darlinghurst, Australia; <sup>e</sup>Department of Medicine, St Vincent's Clinical School, University of NSW, Sydney, Australia

### ABSTRACT

IL-2 is a pleiotropic cytokine that plays an essential role in the survival, expansion, and function of CD8 T cells, regulatory T cells (Tregs), and natural killer (NK) cells. Previous studies showed that binding IL-2 with an anti-IL-2 monoclonal antibody (mAb) with a particular specificity could block its interaction with IL-2R $\alpha$ , which is mainly expressed on Tregs. This selectivity can enhance the anti-tumor effects of IL-2 by activating CD8 T and NK cells, while disfavoring Treg stimulation. Based on this, we newly developed a series of anti-human IL-2 (hIL-2) mAbs (TCB1-3) that selectively stimulate CD8 T and NK cells without overtly activating Tregs. Among them, the hIL-2/TCB2 complex (hIL-2/TCB2c) exerted the best efficacy by inducing a prodigious expansion of host memory phenotype (MP) CD8 T (60-fold) and NK cells (18-fold) with less efficient Treg proliferation (5-fold). As a result, there was an average eightfold increase in the ratio of MP CD8 T to Tregs. Accordingly, hIL-2/TCB2c strongly inhibited the growth of B16F10, MC38, and CT26 tumors. More remarkably, hIL-2/TCB2c showed synergy with checkpoint inhibitors such as anti-CTLA-4 or PD1 antibodies, and resulted in almost complete regression of implanted tumors and resistance to secondary tumor challenge. For direct clinical use, we generated a humanized form of TCB2 that had equal immunostimulatory and anti-tumor efficacy as a murine one. Collectively, these results show that TCB2 can provide a potent immunotherapeutic modality either alone or together with checkpoint inhibitors in cancer patients.

### ARTICLE HISTORY

Received 13 July 2019  
Revised 9 October 2019  
Accepted 11 October 2019

### KEYWORDS

IL-2; TCB2;  
cytokine-antibody complex;  
immunotherapy



### Introduction

IL-2 receptor (IL-2R) is widely expressed on the surface of various lymphoid cells, including CD8 T cells, Foxp3<sup>+</sup> regulatory T (Treg) cells, and natural killer (NK) cells.<sup>1</sup> It is composed of IL-2R $\alpha$  (CD25), IL-2R $\beta$  (CD122), and IL-2R $\gamma$  ( $\gamma_c$ , CD132) subunits, and exists as either  $\alpha\beta\gamma$  heterotrimeric or  $\beta\gamma$  heterodimeric complexes.<sup>2–4</sup> When CD25 binds to IL-2, it induces a conformational change in IL-2 and increases its binding affinity to the IL-2R $\beta$  and IL-2R $\gamma$  to form a tetrameric IL-2/IL-2 receptor complex.<sup>5</sup> In this way, Tregs have 10 to 100-fold higher binding affinity to IL-2. At the steady state, survival of Tregs is dependent on IL-2 and, upon inflammation, Tregs can preferentially bind to soluble IL-2, thereby inhibiting conventional T cell activation.<sup>6</sup>

IL-2 highly stimulates CD8 T and NK cells that can boost anti-tumor immunity, and recombinant human IL-2 (hIL-2), aldesleukin, has been approved for clinical use by the FDA in 1996 and 1992 for the treatment of metastatic melanoma and renal cell carcinoma, respectively.<sup>7</sup> Approximately 10% of

patients showed a durable response, but serious toxic side effects were observed due to the expression of the heterotrimeric IL-2 receptor in lung endothelial cells, which caused fatal vascular leak syndrome.<sup>8–10</sup> Also, IL-2 administration induced a robust Treg expansion that suppressed the anti-tumor activity of CD8 T and NK cells. Moreover, unmodified hIL-2 had an extremely short half-life *in vivo*, further limiting its usage.

One way to circumvent the pitfalls of aldesleukin is to modify IL-2 in a way to extend its *in vivo* lifespan and preferentially direct its effects to CD8 T and NK cells, but not Tregs or endothelial cells. In 2006, Boyman and colleagues reported that when a cytokine is complexed with its antibody, it dramatically increases its *in vivo* half-life and efficacy.<sup>2</sup> Depending on the structure of the complex, it could also be selective for different forms of receptors. For example, anti-IL-2 antibodies such as S4B6 (anti-mouse) and MAB602 (anti-human) can preferentially stimulate CD8 T or NK cells, while JES6-1 (anti-mouse) or 5344 (anti-human) favor the proliferation of Tregs. The recently developed anti-hIL-2 antibody,

**CONTACT** You Jeong Lee  youjeong77@postech.ac.kr  Academy of Immunology and Microbiology, Institute for Basic Science (IBS), Pohang 37673, Republic of Korea

\*The Department of Microbiology and Immunology, Centre for Immunology, University of Minnesota Medical School, Minneapolis, Minnesota, USA.

#Selexcine Inc., Pohang 37666, Republic of Korea

†Deceased

 Supplemental data for this article can be accessed on the [publisher's website](#).

© 2019 The Author(s). Published with license by Taylor & Francis Group, LLC.

This is an Open Access article distributed under the terms of the Creative Commons Attribution-NonCommercial License (<http://creativecommons.org/licenses/by-nc/4.0/>), which permits unrestricted non-commercial use, distribution, and reproduction in any medium, provided the original work is properly cited.

Nara1, can preferentially stimulate the dimeric IL-2 receptor when complexed with hIL-2.<sup>11</sup> Structurally, Nara1 binds near the CD25 binding site of IL-2 and abolishes its binding to IL-2, thereby disfavoring Treg activation.

In this report, we generated anti-hIL-2 antibodies and screened clones that could preferentially work on the dimeric IL-2 receptor by blocking the CD25 binding motif. We selected three clones, named TCB1–3, and found that TCB2 has a unique CDR sequence compared to TCB1, TCB3, and Nara1. The hIL-2/TCB2 complex (hIL-2/TCB2c) had exceptional *in vivo* efficacy in stimulating CD8 T and NK cells, and could inhibit the growth and spread of various tumors such as MC38, CT26, and B16F10. When hIL-2/TCB2c was combined with checkpoint inhibitors such as anti-PD1 or CTLA4 antibodies, tumors were almost completely regressed in mice. Finally, we generated a humanized form of TCB2 that we confirmed to have equal immunostimulatory and anti-tumor effects as a murine one. Collectively, we showed that TCB2 is a new anti-hIL-2 monoclonal antibody (mAb) that has potential therapeutic effects in human cancer patients.

## Material and methods

### Mice

BALB/c, C57BL/6 (B6), Thy1.1 Foxp3-eGFP, mice were maintained at POSTECH Biotech Centre (Korea) under specific pathogen-free condition. For the experiments with anti-tumor effect, B6 or BALB/c mice were purchased from OrientBio (Korea). Unless it is specified, all mice with 6–10 weeks old were used for the experiments according to the protocols approved by the Animal Experimental and Ethic Committee at the Institute for Basic Science (Korea).

### Flow cytometry

Single-cell suspensions were prepared from indicated organs and FACS stained in PBS buffer containing 2% FBS and 0.05% sodium azide. For intracellular staining, single-cell suspensions were surface stained, fixed, and permeabilized with eBioscience Foxp3 staining buffer set. Following antibodies from BD bioscience, BioLegend or ThermoFisher were used for surface or intracellular staining; CD3 (145-2C11), CD4 (GK1.5 or RM4-5), CD8 $\alpha$  (53-6.7), CD25 (PC61), CD44 (IM7), CD62L (MEL-14), CD69 (H1.2F3), CD90.1 (HIS51 or OX-7), CD122 (TM- $\beta$ 1), CD132 (TUGm2), TCR $\beta$  (H57-597), NK1.1 (PK136), Granzyme B (GB11), Foxp3 (MF-14), IFN- $\gamma$  (XMG1.2), NKp46 (29A1.4), CD11b (M1/70), CD27 (LG.7F9), T-bet (4B1D) and pSTAT5 (47/Stat5(pY694)). For pSTAT5 staining, B6 mice were intravenously injected with PBS, hIL-2 (1  $\mu$ g), hIL-2/5344 (1  $\mu$ g/10  $\mu$ g), hIL-2/MAB602 (1  $\mu$ g/10  $\mu$ g) or hIL-2/TCB2 (1  $\mu$ g/10  $\mu$ g) complexes. After RBC lysis using ACK buffer, blood mononuclear cells were fixed with 1.6% PFA (EMS, 25°C) and methanol (DUKSAN, -20°C) for 10 min, respectively, and stained with surface and intracellular markers for 1 h at room temperature.<sup>12</sup> Samples were analyzed using a LSR II or FACSCanto II (BD Biosciences) and analyzed with FlowJo software (Tree Star).

### Generation of anti-hIL-2 mAb producing hybridoma

Immunization of mice and fusion of splenocytes with SP2/0 myeloma cell line (ATCC) was performed as described previously.<sup>13</sup> In brief, splenocytes from BALB/c mice that were immunized with 20–30  $\mu$ g of human IL-2 (hIL-2, Prospec) intraperitoneally for 3–4 times over several weeks were fused with SP2/0 myeloma cell line. Clones were grown in RPMI1640 (Welgene) supplemented with 10% fetal bovine serum (FBS, Atlas Biological), penicillin-streptomycin (Welgene) and hypoxanthine-aminopterin-thymidine (Gibco). Once colonies of hybridoma were visible, the culture supernatants were subjected to ELISA against hIL-2. The positive clones were sub-cloned through serial dilution to ensure that the cell line is the progeny of a single clone.

### Purification of anti-hIL-2 mAbs

Culture supernatant from hybridoma were concentrated by adding 50/45 (v/v) of saturated ammonium sulfate (DAEJUNG) and kept at 4°C for overnight. Precipitates were reconstituted with PBS and then dialyzed for three times against 0.1 M sodium acetate (pH 5.0). Antibodies were purified using protein G resin (GE Healthcare) according to the protocol from the manufacturer.

### Biotinylation of antibodies

Monoclonal antibodies were biotinylated using EZ-Link™ NHS-LC-LC-Biotin (ThermoFisher) according to the protocol from manufacturer.

### Enzyme-linked immunosorbent assay (ELISA)

To check antibody cross-reactivity, mouse or human IL-2 (mIL-2, Peprotech, and hIL-2, Prospec) were plate coated (5  $\mu$ g/ml) overnight and serially diluted anti-hIL-2 (MAB602, R&D systems) or anti-mIL-2 (JES6-1 and S4B6, BioXcell) was applied for 30 min. After washing, anti-mouse or rat IgG-HRP (Southern Biotech) was applied for 15 min, then added tetramethylbenzidine (TMB, Surmodics). The reaction was stopped by adding 2N H<sub>2</sub>SO<sub>4</sub> and OD<sub>450</sub> was measured using microplate photometer. To check binding site competition of MAB602 and TCBs on hIL-2, anti-hIL-2 (clone 5344, BD biosciences) that does not share binding epitope with MAB602 was coated (5  $\mu$ g/ml) overnight. Then, hIL-2 (10ng/ml) was applied for 30 min and serial dilutions of TCBs were applied for 30 min after washing. Biotinylated MAB602 (0.1  $\mu$ g/ml) was added without washing and incubated for 30 min. After washing, Streptavidin-HRP (Thermo Scientific) was added for 15 min followed by TMB reaction. For sandwich ELISA against hIL-2, monoclonal antibodies against hIL-2 were plate coated (2  $\mu$ g/ml) overnight and hIL-2 (10ng/ml) was applied for 30 min followed by biotinylated detection antibodies (0.1  $\mu$ g/ml) for 30 min.

### hIL-2 complex preparation

hIL-2 (500 ~ 1000  $\mu$ g/ml, Genescript) and anti-hIL-2 (500  $\mu$ g/ml) were mixed at 1:10 or indicated molecular ratio and

incubated for 30 min at RT. The complex was diluted in PBS for injection volume (200  $\mu$ l/injection).

### **CTV labeling and adoptive cell transfer of lymphocytes**

Lymph node cells from Thy1.1<sup>+</sup> Foxp3-eGFP<sup>+</sup> mice were labeled with CellTrace Violet (CTV, ThermoFisher) according to the protocol from the manufacturer and then 10<sup>7</sup> cells were intravenously injected on day 0. hIL-2/anti hIL-2 complex was injected daily from day 0 to 3 and then the proliferation of donor cells were measured on day 5.

### **CTLL2 cell proliferation assay**

CTLL2 cell line was purchased from ATCC and cultured in the presence of indicated serum for 2 days. The proliferation of CTLL2 cells was analyzed with CellTiter 96<sup>®</sup> Non-Radioactive Cell Proliferation Assay (MTT, Promega) according to the manufacturer's protocol.

### **Affinity measurement for anti-hIL-2 mAbs**

Nine hundred RU (Rmax = 90) of MAB602, 5344 or TCB2 (produced from serum-free media) were immobilized on CM5 chip (GE healthcare) by amine reaction. A twofold serial dilution of hIL-2 starting at 100 nM was pulsed for 3 min at 10  $\mu$ l/min and then dissociation of hIL-2 was chased for 10 min. The surface plasmon resonance curve was obtained using Biacore T100 (GE healthcare) or Biacore T200 at Postech (Pohang, Korea) or Unist (Ulsan, Korea), respectively.

### **CDR region sequencing of anti-hIL-2 mAbs**

CDR region of antibody heavy chain and light chain sequencing was performed as previously described.<sup>14</sup> In brief, RNA was isolated from 5  $\times$  10<sup>6</sup> hybridoma cell line using TRIzol (ThermoFisher) according to the protocol from the manufacturer. cDNA was synthesized using QuantiTect Reverse Transcription Kit (Qiagen) according to the protocol from manufacturer. PCRs for the variable region of light chain and heavy chain were performed as previously described.<sup>14</sup> The PCR products were cloned into TA vector (ThermoFisher) and then DNA sequencing was performed at Cosmogenetech.

### **Production of recombinant human-chimeric and humanized TCB2**

Antibody humanization was performed in GenScript (USA) and cloned into a human IgG1 backbone. Humanized TCB2 (hTCB2) were expressed using ExpiCHO Expression System (ThermoFisher) according to the protocol from manufacturer. Purification of antibody was performed with protein G resin with purity more than 95%.

### **Tumor models**

B16F10, MC38, and CT26 cell lines were purchased from ATCC. For all tumor experiments, we injected reagents into mice with a measurable tumor mass. B16F10 cells (1  $\times$  10<sup>6</sup>)

were subcutaneously injected into B6 mice on day 0 and PBS, hIL-2 alone (1.5  $\mu$ g), hIL-2/TCB1 (0.8  $\mu$ g/8  $\mu$ g) or hIL-2/TCB2 (0.8  $\mu$ g/8  $\mu$ g) complex were daily injected intraperitoneally from day 4 to 7. Trp2<sub>180-188</sub> [SVYDFVWL] (100  $\mu$ g, Peptron) and poly:IC (100  $\mu$ g, Invivogen) were injected on day 3 and 10 and hIL-2/TCB2c daily injected from day 4 to 7 and day 11 to 14.<sup>15</sup> The systemic tumor model was generated by intravenously injecting B16F10 cells (3  $\times$  10<sup>5</sup>) as previously described.<sup>8</sup> For the anti-CTLA4 and hIL-2/TCB2c co-treatment experiment, CT26 cells (5  $\times$  10<sup>5</sup>) were subcutaneously injected into BALB/c mice and injected with anti-mouse CTLA4 (UC10-4F10-11, BioXcell, 100  $\mu$ g, on day 7, 9 and 11) and/or hIL-2/TCB2 complex (0.8  $\mu$ g/8  $\mu$ g on day 8, 9, 10 and 11) after tumor inoculation. For testing synergistic anti-tumor response of anti-PD-1 and hIL-2/TCB2c, MC38 cells (5  $\times$  10<sup>5</sup>) were subcutaneously injected into B6 mice, which were injected with anti-mouse PD-1 (29F.1A12, BioXcell, 100  $\mu$ g, on day 7, 10 and 13) and/or hIL-2/TCB2 complex (0.8  $\mu$ g/8  $\mu$ g, day 8, 9, 10, 11) after tumor inoculation. To test the anti-tumor memory response, MC38 cells (5  $\times$  10<sup>5</sup>) were injected to tumor cured or naïve B6 mice. Tumor-bearing mice were sacrificed when the tumor size reaches 800 mm<sup>3</sup>.

### **Ethics statement**

This research was approved by the Institutional Animal Care and Use Committees (IACUC) of the Pohang University of Science and Technology (2013-01-0012). Mice care and experimental procedures were performed in accordance with all institutional guidelines for the ethical use of non-human animals in research and protocols from IACUC of the Pohang University of Science and Technology.

## **Results**

### **Development of new anti-hIL-2 antibodies**

To develop a new anti-hIL-2 antibody that can selectively stimulate CD8 T or NK cells when complexed with hIL-2 *in vivo*, we immunized BALB/c mice with hIL-2 and screened antibodies under two criteria: first, it binds to human, but not mouse IL-2; second, its binding to hIL-2 is blocked by MAB602, but not by 5344. Although the binding epitope of MAB602 and 5344 have not yet been analyzed, we assumed that the former and the latter block CD25 and CD122/CD132 binding sites, respectively, based on a structural analysis of their respective functional counterparts of mouse antibodies, S4B6 and JES6-1.<sup>16</sup> After the vigorous screening, we generated three anti-hIL-2 antibody clones named TCB1, TCB2, and TCB3. These clones were only reactive to hIL-2, whereas MAB602 reacted mouse IL-2 (mIL-2) to some extent as previously shown<sup>11</sup> (Figure S1A). In ELISA, when hIL-2 was first treated with either TCB1-3 or MAB602, the binding of other antibodies of these could be completely blocked, indicating that these four antibodies have significant overlap in their epitopes and cause steric hindrance (Figure S1B and C). We sequenced the CDR regions of TCB1-3 and compared them with those of Nara1, which has been previously known to block the CD25 binding site of hIL-2.<sup>11</sup> Interestingly, the

CDRs of TCB1 and TCB3 had about 80% sequence homology with those of Nara1, suggesting that they might share a common binding epitope (Table 1). However, TCB2 had unique CDRs, and their sequence similarities with Nara1 were 34% in average. Collectively, these results show that TCB2 is a new anti-hIL-2 antibody that is different from Nara1 and shares a common binding epitope with MAB602.

### ***hIL-2/TCB2c selectively stimulates CD8 T and NK cells while relatively disfavoring treg activation***

To test the *in vivo* activity of hIL-2/TCBc in mouse, we transferred CellTrace Violet (CTV)-labeled donor lymph node (LN) cells isolated from Thy1.1 Foxp3-eGFP mice to a congenic host and injected hIL-2/TCBc. As shown in Figure 1a, 1.5 µg of hIL-2 alone was not sufficient to drive CD8 T cell proliferation. However, 0.8 µg of hIL-2 complexed with 8 µg of TCBs, especially hIL-2/TCB2c, induced robust donor T cell activation in terms of CTV dilution, CD44 upregulation, and granzyme B secretion (Figure 1a,b). Herein, we chose TCB2 for further development and analyzed its effects on the host immune cells (Figure 2). hIL-2/TCB2c induced vigorous proliferation of CD8 T (60-folds) and NK (18-folds) cells while relatively disfavoring Treg expansion (5-folds) (Figure 2a,b). After four consecutive injections of hIL-2/TCB2c, the numerical ratio of memory phenotype (MP) CD8 T cells or NK cells to Tregs increased eight- and fivefold, respectively. NK cells are classified into four main developmental stages based on the expression of CD11b and CD27; most immature CD11b<sup>-</sup>CD27<sup>-</sup> cells matured sequentially into CD11b<sup>-</sup>CD27<sup>+</sup>, CD11b<sup>+</sup>CD27<sup>+</sup>, and CD11b<sup>+</sup>CD27<sup>-</sup> cells.<sup>17,18</sup> Upon hIL-2/TCB2c injection, all four subsets of NK cells expanded with upregulation of activation marker CD69,<sup>19</sup> particularly in CD11b<sup>+</sup> populations, which had high cytotoxic activity<sup>20</sup> (Figure 2c,d). The effect of T cell proliferation after hIL-2/TCB2c injection lasted for more than 2 weeks after injection and the increased memory cell proportion persisted for more than a month (Figure S2). Therefore, hIL-2/TCB2c selectively expanded and activated CD8 T and NK cells for extended periods.

### ***hIL-2/TCB2c provides prolonged IL-2 receptor stimulation to MP CD8 T cells, which express the highest level of heterodimeric IL-2 receptor***

As phosphorylation of STAT5 protein is a downstream event of IL-2 receptor engagement,<sup>21</sup> we measured its expression in T cells and used it as a readout of signal intensity of IL-2. hIL-2 complexed with 5344, MAB602, or TCB2 were intravenously

(IV) injected and pSTAT5 upregulation on circulating CD8 T, NK and Tregs were analyzed 20 or 180 min later (Figure 3a,b). As expected, hIL-2 alone, hIL-2/MAB602c, and hIL-2/TCB2c uniformly upregulated pSTAT5 on CD8 T cells and Tregs 20 min after injection (Figure 3a). Due to its short half-life, hIL-2 alone resulted in relatively short-lived upregulation of pSTAT5 on CD8 T cells that disappeared after 180 min. However, its effect lasted beyond 180 min after injection when complexed with its antibodies. Interestingly, pSTAT5 was upregulated in NK cells only when IL-2 was injected in complex form 180 min after injection, but not at 20 min later (Figure 3a,b). We found the pSTAT5 level was higher in T cells injected with hIL-2/TCB2c than with hIL-2/MAB602c (Figure 3a,b), indicating that the former has a longer *in vivo* half-life. When we analyzed the *in vitro* survival of the CTLL2 cell line, which is dependent on IL-2 for survival, it was estimated that hIL-2/TCB2c had about a 48-h half-life in the serum (Figure S3). This is significantly longer than that of hIL-2/MAB602c, which has about a 36-h half-life. Clone 5344, like JES6-1, worked only on Tregs as expected (Figure 3a,b).<sup>8</sup> On Tregs, all complexes worked equally well at the 20 and 180-min time points. This could be due to the stability of the heterotrimeric IL-2 receptor complex on Tregs. As a result, the pSTAT5 mean fluorescent intensity (MFI) ratio of CD8/Treg was the highest with hIL-2/TCB2c (Figure 3a,b, right). To explain why IL-2 works best on MP CD8 T cells when antibody interferes with CD25 binding, we analyzed the expression patterns of IL-2 receptor subunits on T cells (Figure 3c,d). Only Tregs expressed CD25, but they had an intermediate level of CD122 expression; on the other hand, MP CD8 T cells expressed the highest levels of CD122 (Figure 3c). Although CD132 was slightly higher in Tregs, this result explains how MP CD8 T cells outcompete Tregs and CD4 T cells when CD25 is not able to engage IL-2.

### ***hIL-2/TCB2c has better *in vivo* efficacy than hIL-2/MAB602c***

The binding epitope on IL-2 for the anti-IL-2 mAb seems to be a major factor determining the functional heterogeneity of the IL-2 cytokine-antibody complex.<sup>2,16</sup> However, the previous results suggested that the affinity of antibodies could also influence the quality of T cell subset stimulation. To address this, we measured the affinity of anti-hIL-2 mAbs for hIL-2 using surface plasmon resonance (Figure S4). The hIL-2 binding curve was slightly (16.7%) higher with TCB2 than with MAB602, and the dissociation rate was much slower (44.1%) for TCB2 than for MAB602. Overall, the affinity of MAB602 for hIL-2 was expected to be 38% of that of TCB2. The binding pattern of 5344 to hIL-2 was different

**Table 1.** TCB2 has unique CDR sequences.

CDRs	Amino acid sequence				Sequence homology with Nara1 (%)		
	Nara 1	TCB1	TCB2	TCB3	TCB1	TCB2	TCB3
κ1	KASQSVVDYDGDSSYMN	KASQSVVDYDGDSSYMN	ITSTDID DDMN	KASQSVVDYDGDSSYMN	100	<b>27</b>	100
κ2	AASNLES	AASNLES	EGNTRP	AASNLES	83	<b>14</b>	100
κ3	QQSNEPWT	QQSNEPWT	LQSDNLPYT	QQSNEPWT	89	<b>56</b>	89
H1	NYLIE	NYLIE	TYWIQ	NYLIE	100	<b>40</b>	100
H2	VINPGSGGTNYNEKFKG	VINPGSGGTNYNEKFKG	AIYPGDGDRYIQNFKG	VINPGSGGSNYNEKFKG	100	<b>53</b>	94
H3	WRGDGYAYFDV	DYGLHRLDY	SLATRGFYAMDY	WDFGYAMDY	8	<b>17</b>	17
Ave					80	<b>34</b>	83

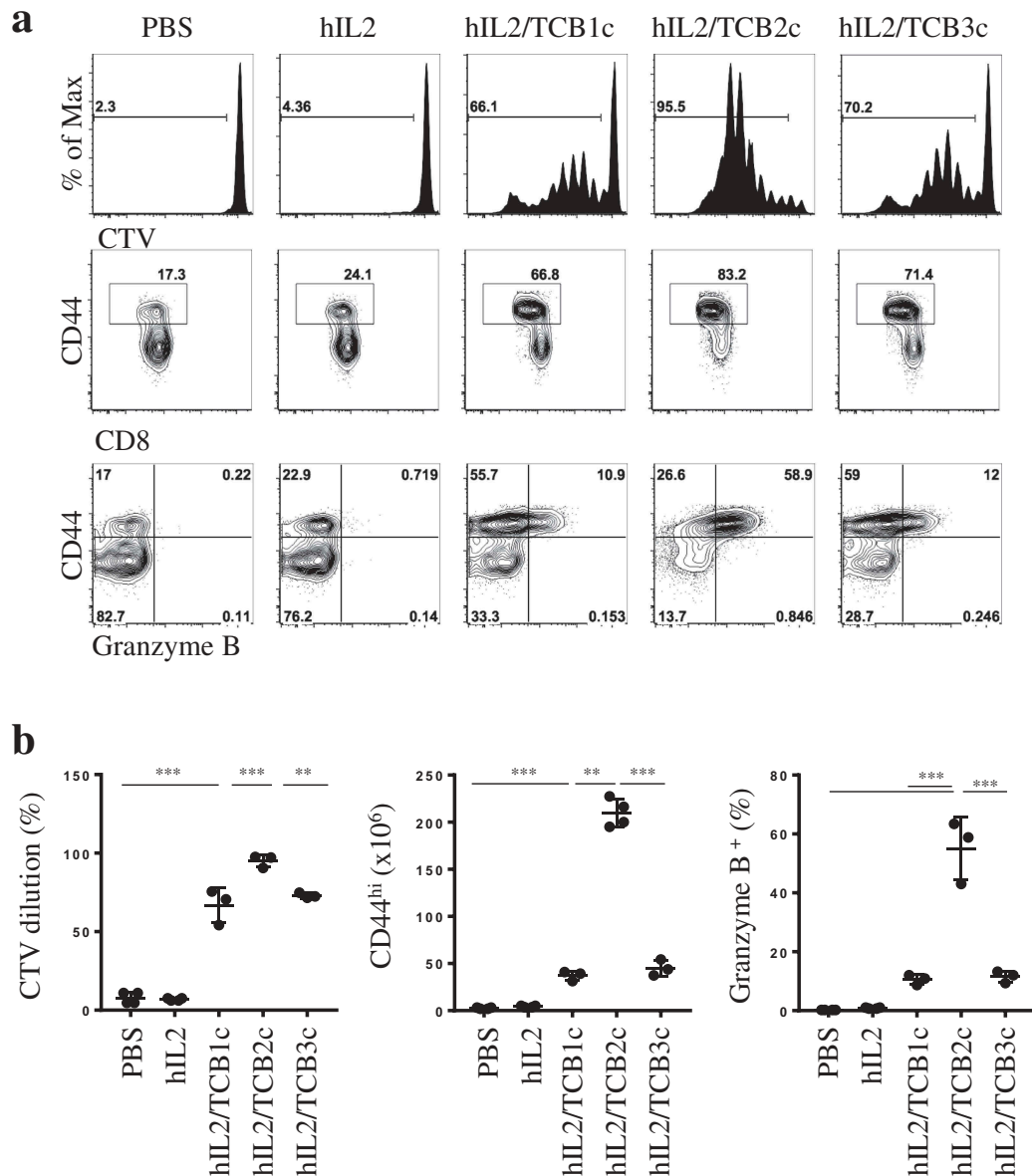


**Figure 1.** Generation of anti-human IL-2 antibodies that stimulate CD8 T cells as a cytokine-antibody complex.

B6 mice were injected with CellTrace violet (CTV) labeled lymph node cells from Thy1.1<sup>+</sup> Foxp3-eGFP<sup>+</sup> mice on day 0, followed by daily injections with hIL-2 (1.5  $\mu$ g) or indicated antibody complexes (0.8  $\mu$ g/8  $\mu$ g) from day 0 to 3. The proliferation, activation and granzyme B expression of CD8 T cells in the spleen were analyzed on day 5 by flow cytometry. (a) Representative histograms and dot plots are shown. Numbers indicate the frequency of cells in adjacent gates or regions. (b) Graphs show the statistical analysis of proliferation, memory phenotype (CD44<sup>hi</sup>) acquisition and granzyme B secretion of splenic CD8 T cells. Each dot represents individual mouse and horizontal bars indicate mean values. Error bars indicate standard deviation (SD). \* $p$  < .05; \*\* $p$  < .01; \*\*\* $p$  < .001 (one-way ANOVA). hIL-2/TCB2c, human IL-2/TCB2 complex. A representative result is shown from three independent experiments using 3-4 mice per group.

from that of MAB602 and TCB2, suggesting that it might have a different mode of interaction with hIL-2. Next, we tested if the prolonged *in vivo* half-life (Figure 3) and *in vitro* affinity (Figure S4) of hIL-2/TCB2c compared to hIL-2/MAB602c can drive better immune cell response. Two-fold serial dilutions of hIL-2/TCB2c or hIL-2/MAB602c were intraperitoneally injected into mice for four consecutive days and T cell proliferation was measured 48 h after the last injection (Figure 4). The number of MP CD8 T cells was higher in the hIL-2/TCB2c-injected group than in the hIL-2/MAB602c-injected group, while the number of Tregs was not significantly different between them (Figure 4). As a result, 0.8/8  $\mu$ g injection of hIL-2/TCB2c and hIL-2/MAB602c induced average 7.7 and 3.7-fold increases in MP CD8/Treg numbers ratio, respectively (Figure 4b, right). Furthermore, hIL-2/TCB2c induced

stronger NK expansion (Figure S5A, right), as well as more granzyme B (Figure S5B) and IFN $\gamma$ -producing (Figure S5C) CD8 T cells in the spleen. Collectively, we showed that hIL-2/TCB2c has a higher affinity and longer half-life than hIL-2/MAB602c, and it induced a more robust CD8 T and NK cell response.

### ***hIL-2/TCB2c enhances anti-tumor immunity and synergizes with the peptide-based tumor vaccine and checkpoint inhibitor***

To demonstrate the potential clinical utility of the TCB2 mAb against human cancer patients, we established a malignant melanoma model using B6 mice inoculated with B16F10 cells subcutaneously. Then, the mice were injected with PBS, hIL-2 alone,

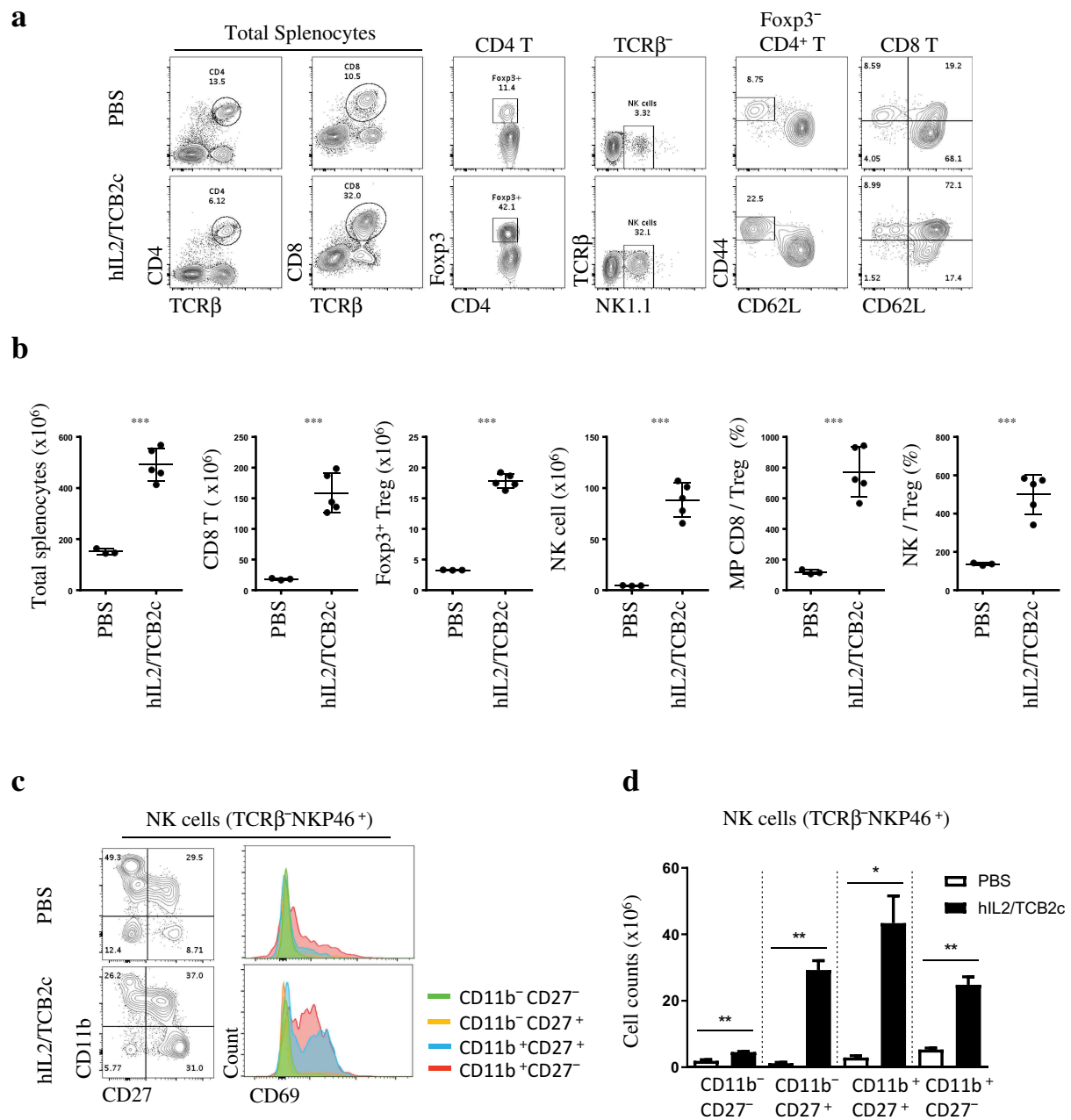


**Figure 2.** hIL-2/TCB2c selectively stimulates CD8 T and NK cells while relatively disfavoring Treg activation.

B6 mice were daily injected with PBS or hIL-2/TCB2c (0.8  $\mu$ g/8  $\mu$ g) from day 0 to 3 and splenocytes were analyzed on day 5. (a and c) Single-cell suspension of splenocytes were stained with indicated markers and analyzed by flow cytometry. Representative dot plots are shown and numbers indicate the frequency of cells in adjacent gates or each quadrant. (b and d) Graphs shows numbers or frequencies of indicated populations with statistical analysis (N = 3 ~ 5). Each dot represents individual mouse and horizontal bars indicate mean values. Error bars indicate standard deviation (SD). \* $p$  < .05; \*\* $p$  < .01; \*\*\* $p$  < .001 (unpaired  $t$ -test). hIL-2/TCB2c, human IL-2/TCB2 complex. A representative result is shown from four (a and b) and 2 (c and d) independent experiments.

hIL-2/TCB1c or hIL-2/TCB2c from day 4 to 7, and tumor progression was monitored for the next 7 days (Figure 5a). As expected, tumor growth was most strongly inhibited by treatment with hIL-2/TCB2c, followed by with hIL-2/TCB1 complex and with hIL-2 alone. This result is well correlated with the observed magnitude of CD8 T cell expansion (Figure 1). Next, we tested the effect of TCB2 in a systemic tumor model using B6 mice that were IV injected with B16F10 melanoma cells (Figure 5b). The mice were injected daily with hIL-2/TCB2c from day 4 to 7 and then the number of pulmonary

tumor nodules was measured on day 18. Similar to the solid B16F10 model, we observed hIL-2/TCB2c most significantly suppressed the growth of pulmonary tumor nodules.

We further tested if hIL-2/TCB2c has synergistic effects with other anti-tumor therapies, such as T cell stimulation with tumor neo-antigen<sup>15,22</sup> and checkpoint inhibitors<sup>23,24</sup> B6 mice were subcutaneously injected with B16F10 melanoma cells and injected with PBS or Poly I:C plus TRP2 peptide<sup>15</sup> as indicated (Figure 5c). TRP2 peptide or hIL-2/TCB2c significantly delayed the growth of B16F10 tumor; however,

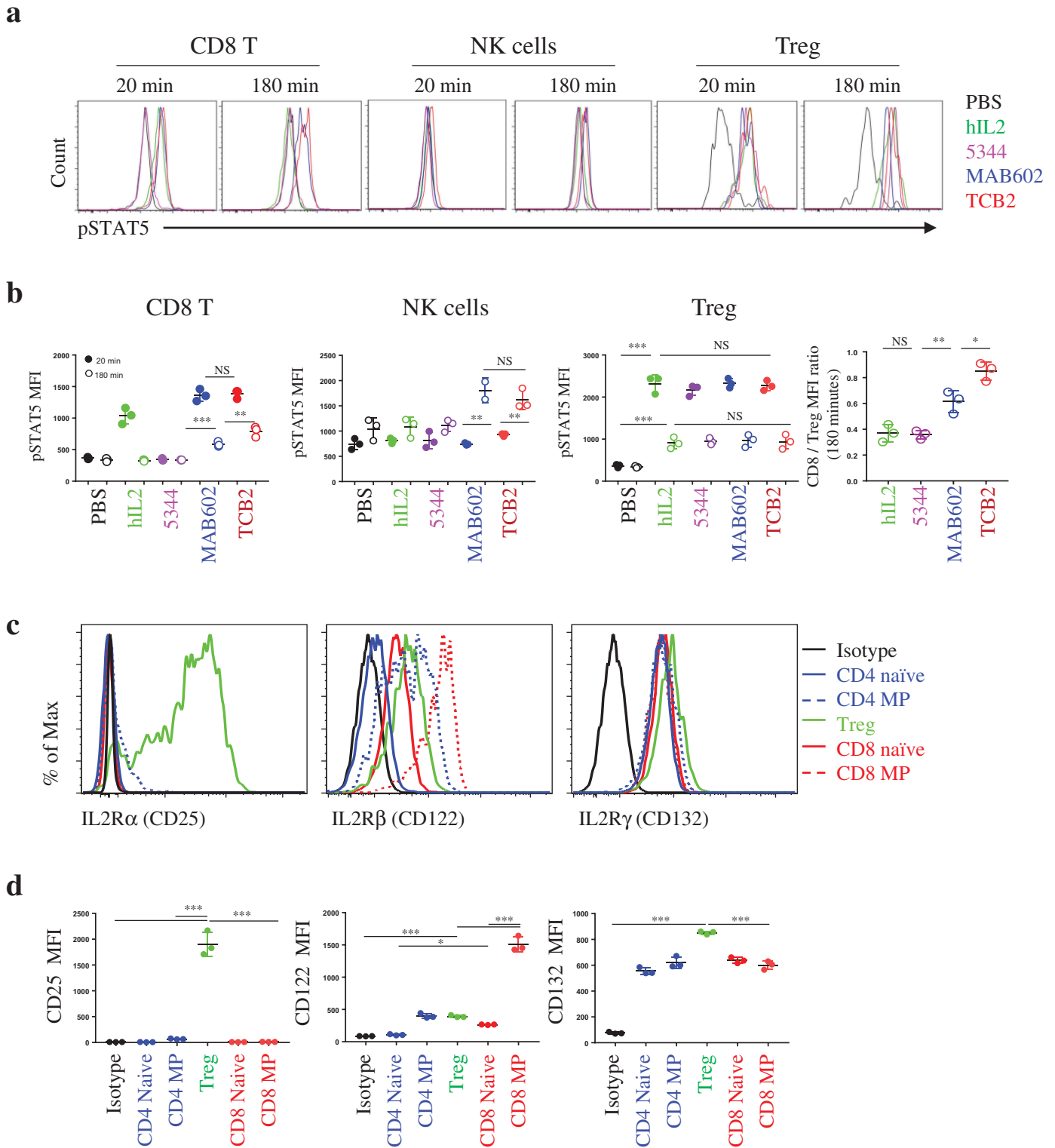


**Figure 3.** hIL-2/TCB2c provides prolonged IL-2 receptor stimulation to MP CD8 T cells, expressing the highest level of heterodimeric IL-2 receptor.

(a and b) B6 mice were injected with PBS, hIL-2 (1  $\mu$ g) or hIL-2/TCB2c (1  $\mu$ g/10  $\mu$ g) once and pSTAT5 in lymphocytes were analyzed after 20 and 180 min. Representative histograms show pSTAT5 expression in CD8 T, NK and regulatory T cells (a). Statistical analysis of pSTAT5 MFIs of indicated cell types and their ratios are shown (N = 3) (b). (c and d) Representative histograms show surface expression of IL-2 receptor subunits in indicated cell types (c) and statistical analysis of MFIs of IL-2 receptor subunits are shown (N = 3) (d). Each dot represents individual mouse and horizontal bars indicate mean values. Error bars indicate standard deviation (SD). MFI, mean fluorescence intensity; \* $p$  < .05; \*\* $p$  < .005; \*\*\* $p$  < .001 (one-way ANOVA); hIL-2/TCB2c, human IL-2/TCB2 complex; NS, not significant. Representative result is shown from three independent experiments.

when TRP2 peptide was used in combination with hIL-2/TCB2c, the anti-tumor effect was further enhanced. Next, we tested the synergistic anti-tumor effect of anti-PD1 with

hIL-2/TCB2c using a suboptimal dose of anti-PD-1 that could not elicit an anti-tumor response, thus mimicking the clinical condition wherein anti-PD1 therapy is not fully effective



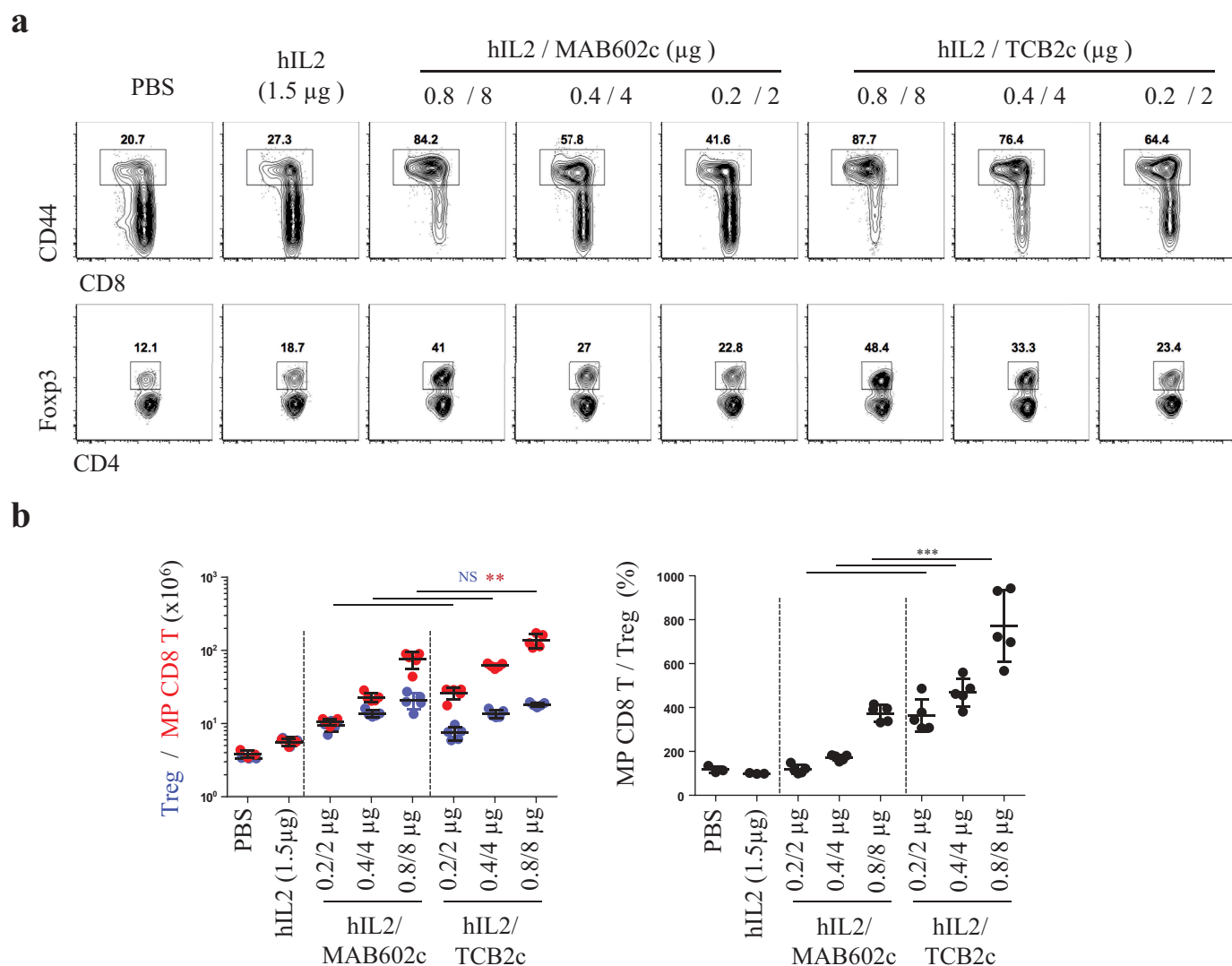


**Figure 4.** hIL-2/TCB2c has better *in vivo* efficacy than hIL-2/MAB602c.

Indicated doses of hIL-2/MAB602c or hIL-2/TCB2c were daily injected into B6 mice from day 0 to 3 and splenic T cell activation was analyzed on day 5 by flow cytometry. (a) Representative dot plots show frequencies of CD44<sup>hi</sup> cells in total CD8 T cells (upper panels) and Tregs in total CD4 T cells (lower panels). Numbers indicate the frequency of cells in adjacent gates. (b) Graphs show statistical analysis of absolute numbers of memory phenotype (MP) CD8 T cells (red) and Tregs (blue) and their numerical ratios in the spleen (right). Pooled results from two independent experiments are shown. Each dot represents individual mouse and horizontal bars indicate mean values. Error bars indicate standard deviation (SD); \* $p < .05$ ; \*\* $p < .01$ ; \*\*\* $p < .001$  (one-way ANOVA); hIL-2/MAB602c, human IL-2/MAB602 complex; hIL-2/TCB2c, human IL-2/TCB2 complex. A representative result is shown from two independent experiments using three mice per group.

(Figure 5d). Consistent with the result from B16F10 tumors, hIL-2/TCB2c alone could significantly delay MC38 tumor growth and eradicated tumors in 3 out of 8 mice (37%) (Figure 5d). Remarkably, when a suboptimal dose of anti-PD1 antibody was combined with hIL-2/TCB2c, it completely rejected tumors in all 7 mice (Figure 5d). We also tested if tumor-free mice would become resistant to secondary tumor challenge. At day 25, MC38 tumor cells were re-inoculated in tumor-free mice from the hIL-2/TCB2c ( $N = 3$ ) or hIL-2/TCB2c plus anti-PD1 mAb-treated ( $N = 7$ ) groups (Figure 5d). Surprisingly, tumors did not grow again in any of these mice that rejected the first tumor. The synergistic anti-tumor response was also observed in a CT26 colon tumor model treated with an anti-CTLA4 antibody (Figure S6). Collectively, these results demonstrate that TCB2 is a potent anti-hIL-2 mAb that has a therapeutic potential for cancer

immunotherapy when used as hIL-2/TCB2c alone, or in combination with checkpoint blockers or a tumor vaccine.

### Humanized form of TCB2 provides effective anti-tumor immunity

For the therapeutic application of TCB2 in humans, we generated various forms of humanized TCB2 (hTCB2) and selected a clone that has about 70% the affinity of that of a murine one (Figure 6a and Table S1). We compared the efficacy of T cell stimulation of TCB2 in B6 mice that were injected with either hIL-2/TCB2c or hIL-2/hTCB2c (Figure 6b) and found the expansion of CD8 T, NK, and Treg cells were comparable (Figure 6b). Finally, to confirm that the anti-tumor response is preserved in hTCB2, B6 mice were subcutaneously inoculated with MC38 cells and injected with anti-PD1 in combination with either hIL-2/hTCB2c or hIL-2/

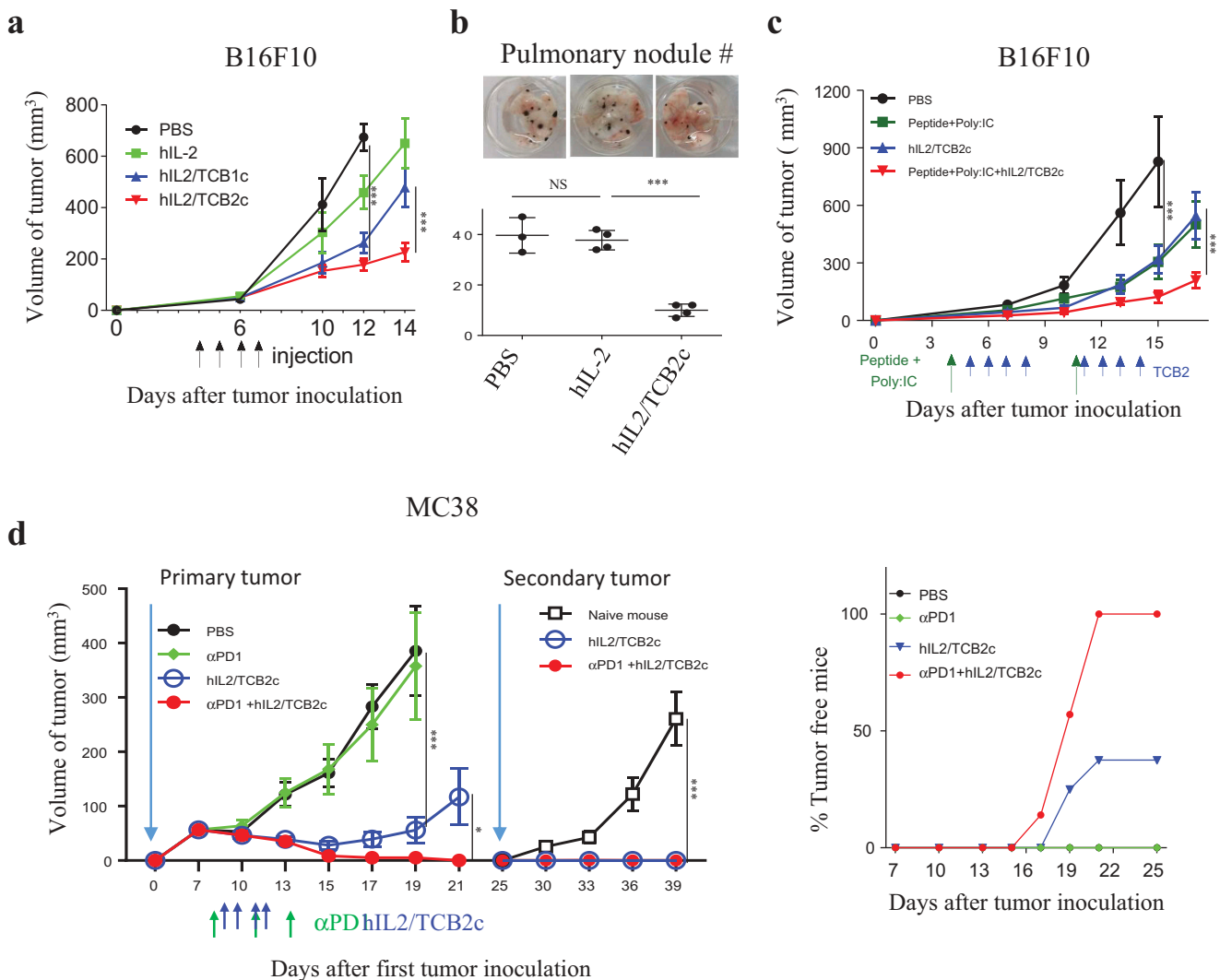


**Figure 5.** hIL-2/TCB2c enhances anti-tumor immunity and synergizes with peptide-based tumor vaccine and a checkpoint inhibitor.

(a) B6 mice were subcutaneously inoculated with B16F10 melanoma cells on day 0 and daily injected with hIL-2/TCB1c (0.8 μg/8 μg) or hIL-2/TCB2c (0.8 μg/8 μg) from days 4 to 7. Tumor growth was monitored until day 14 (N = 8 ~ 10). \*\*\**p* < .001 (Two-way ANOVA for day 12, unpaired *t* test for day 14). (b) B6 mice were intravenously injected with B16F10 melanoma cells on day 0 and daily injected with hIL-2 (0.8 μg) or hIL-2/TCB2c (0.8 μg/8 μg) from days 4 to 7. Pictures show representative lung specimen (top) and a graph shows a statistical analysis of the number of pulmonary tumor nodules on day 18 (N = 3 ~ 4, bottom). Each dot represents individual mouse and horizontal bars indicate mean values. Error bars indicate standard deviation (SD). \*\*\**p* < .001 (One-way ANOVA); NS, not significant. (c) B6 mice were subcutaneously inoculated with B16F10 melanoma cells on day 0 and injected with either PBS, Trp2 peptide (100 μg) plus Poly:IC (100 μg), hIL-2/TCB2c (0.8 μg/8 μg) or Trp2 peptide (100 μg) plus Poly:IC (100 μg) with hIL-2/TCB2c (0.8 μg/8 μg) on indicated days. Graph shows tumor progression measured thereafter [N = 6 (PBS), N = 8 (peptide+Poly:IC), N = 7 (hIL-2/TCB2c), N = 10 (peptide+Poly:IC+hIL-2/TCB2c)]. (D) B6 mice were subcutaneously inoculated with MC38 colon cancer cells on day 0 and injected with PBS or suboptimal dose of anti-PD1 (100 μg) and/or hIL-2/TCB2c (0.8/8 μg) as indicated (N = 6 ~ 8). At day 25, tumor-free mice (N = 3 for hIL-2/TCB2c and N = 7 for anti-PD1 + hIL-2/TCB2c) were inoculated again with MC38 cells and tumor progression was monitored until day 42. Graphs shows tumor volume (left) and percentage of tumor-free mice (right). Error bars indicate standard error of mean (SEM). \**p* < .05; \*\*\**p* < .001 (One-way (b) and Two-way (a, c, and d) ANOVA). hIL-2/TCB2c, human IL-2/TCB2 complex. Representative result is shown from three independent experiments.

TCB2c (Figure 6c). In this experiment, the mice were injected with an optimal dose of anti-PD1 (200 μg/injection) to compare the full efficacy of tumor growth inhibition (Figure 6c). As expected, tumor growth was significantly inhibited by both anti-PD1 antibody alone and hIL-2/hTCB2c complex alone, and the rejection rate was 25% and 40%, respectively. Remarkably, injection with anti-PD1 in combination with either hIL-2/TCB2c or IL-2/hTCB2c resulted in complete regression of tumors by 100% (7 out of 7) and 90% (8 out of 9), respectively, by day 25 after tumor graft (Figure 6c). These results indicate that hTCB2c has comparable *in vivo* efficacy with the murine form of TCB2.

## Discussion

In this report, we showed that hIL-2/TCB2c preferentially stimulates CD8 T and NK cells, while relatively disfavoring Treg expansion. Although we are still analyzing the molecular structure of hIL-2 and TCB2 complex, these functional properties are likely due to the blocking of the CD25 binding motif of hIL-2 by TCB2. Tregs expressed an intermediate level of heterodimeric IL-2Rβγ and, therefore, in the absence of CD25 binding ability, IL-2 favored MP CD8 T cells, which express the highest level of IL-2Rβγ (Figure 3c). When the mice were injected with hIL-2 alone or hIL-2 antibody complexes,

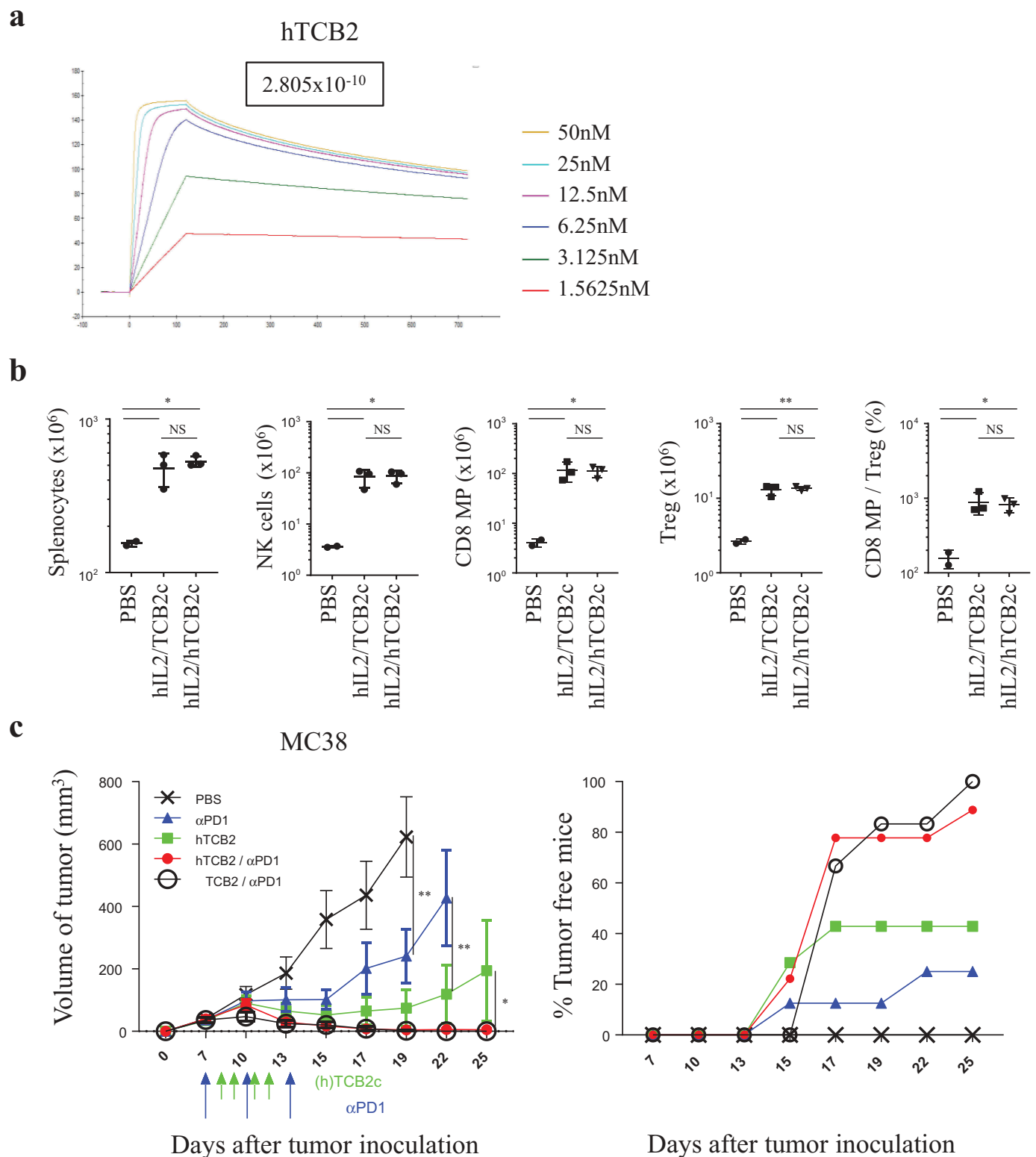


**Figure 6.** Humanized form of TCB2 provides effective anti-tumor immunity.

(a) Figure shows the results of surface plasmon resonance for binding of fully humanized TCB2 (hTCB2) to hIL-2. (b) B6 mice were daily injected with PBS, hIL-2/TCB2c (0.8  $\mu$ g/8  $\mu$ g) or hIL-2/hTCB2c (0.8  $\mu$ g/8  $\mu$ g) from day 0 to 3 and splenic T cells were FACS analyzed on day 5. Graphs show numbers of indicated cells and ratios. Each dot represents individual mouse and horizontal bars indicate mean values (N = 2 ~ 3). Error bars indicate standard deviation (SD). (c) B6 mice were subcutaneously inoculated with MC38 cells on day 0 and injected with PBS, anti-PD1 (200  $\mu$ g/injection) and/or hIL-2/TCB2c or hIL-2/hTCB2c (0.8/8  $\mu$ g, N = 7 ~ 9) as indicated. Graphs shows tumor volume (left) and percentage of tumor-free mice (right). Error bars indicate standard error of mean (SEM). \* $p$  < .05; \*\* $p$  < .01 (Two-way ANOVA (day 19/22) and unpaired  $t$  test (day 25); NS, not significant). hIL-2/TCB2c, human IL-2/TCB2 complex. Shown are the result of two (a and b) or three (c) independent experiments.

pSTAT5 expressions in CD8 T cells were proportional to their proliferation capacity, suggesting pSTAT5 faithfully report signaling intensity of IL-2R $\beta\gamma$  complex (Figure 3a,b). Interestingly, Tregs had a similar pattern of pSTAT5 expression regardless of the hIL-2 formulation and NK cells showed a delayed response with pSTAT5 upregulation. One possible explanation is that a small amount of IL-2 released from the complex and captured by CD25, which is constitutive on Tregs and inducible on NK cells with cytokine stimulation such as IL-12 and IL-18.<sup>25</sup> This might be enough for the phosphorylation of STAT5 in Tregs, but not for their proliferation. However, this does not explain overt NK cell activation and proliferation by hIL-2/TCB2c after repetitive injections (Figure 2). There may be more complex cytokine storms after administration of IL-2 and further investigations are required to understand the heterogeneous response of each cell type.

There are several recently developed IL-2-mediated anti-tumor drugs, such as neoleukin-2/15<sup>17</sup> anti-hIL-2 (Nara1),<sup>11</sup> IL-2 superkine,<sup>26</sup> CEA-IL-2v<sup>27</sup>, and NKTR-214.<sup>28,29</sup> IL-2 superkine is a selected mutant that had increased affinity for IL-2R $\beta$  without CD25, and neoleukin-2/15 is designed mimics of IL-2 that has decreased affinity to CD25, thereby working better on CD8 T cells than Tregs. Similarly, CEA-IL-2v is an anti-CEA antibody linked with a variant of hIL-2 that has a mutated CD25 binding site, thereby recruits CD8 T cells to tumor cells that express CEA antigen. However, these mutation-based approaches could potentially render the modified IL-2 immunogenic and/or susceptible to proteolytic enzymes that degrade artificially introduced amino acid sequences. NKTR-214 is a prodrug of hIL-2 that is PEGylated on the CD25 binding site, in which six PEG residues are slowly released to make an active and stable form of hIL-2. As PEG molecules block the CD25 binding motif, it preferentially activates heterodimeric IL-2 receptors over heterotrimeric complexes.<sup>28–30</sup> These properties rendered hIL-2 to have increased serum half-life without overt Treg activation and toxic side effects. This mode of action, however, could possibly induce continuous IL-2 signaling on T cells with low levels of stimulation, as most active forms are not stable and most stable forms are not active. In contrast, hIL-2/TCB2c does not require an activation step and is stable. We also noticed that four consecutive high-dose injections of hIL-2/TCB2 (0.8  $\mu$ g/8  $\mu$ g) had an equal or better anti-tumor effects compared with seven consecutive low-dose injections (0.6  $\mu$ g/6  $\mu$ g), although the total amount of IL-2 was higher in the latter (Figure S7). This finding may suggest that there is a certain threshold for IL-2 signaling required for optimal T cell activation. We estimated from the literature that, for the mouse *in vivo* usage, 0.160–0.320 mg/kg of TCB2 was comparable with 2 mg/kg of NKTR214 and 4 mg/kg of IL-2 superkine. As a result, we showed that hIL-2/TCB2c could inhibit tumor growth in mouse models of malignant melanoma (B16F10) and colon cancer (MC38 and CT26) (Figure 5 and S6). Also, hIL-2/TCB2c showed synergy with checkpoint blockers such as anti-PD1 and anti-CTLA4 similar to previous reports.<sup>28,31,32</sup>

We showed that TCB1, TCB3, and Nara1 share similar CDR sequences, but TCB2 has a unique one. It was quite surprising that TCB1, TCB3 and Nara1, which were

developed in different sets of experiments, had high homology in their CDR sequences. We speculate that CD25 binding epitope on hIL-2 is very restricted, and there is not many chances for having different CDRs for efficient binding. IL-2 epitopes of TCB antibodies overlap with each other, and it is possible that TCB2 directly binds to the CD25 recognition motif, rather than binding to its adjacent area and provide steric hindrance as shown in Nara1.<sup>11</sup> To address this issue, we are analyzing the detailed structure of the hIL-2/TCB2c by X-ray crystallography, which will reveal the precise mode of binding by TCB2 to hIL-2.

For human clinical application, we generated a humanized form of TCB2 and confirmed that it has similar anti-tumor effects and is ready for clinical trials (Figure 6). To minimize Treg activation by IL-2 released from the complex, as well as make it easier and cheaper for mass production, we are currently generating a single chain complex wherein hIL-2 and TCB2 are connected by a linker sequence.

When the anti-IL-2 antibody interferes CD122 binding, it can be used to expand Tregs as seen in clone 5344 (anti-human IL-2) and JES6-1 (anti-mouse IL-2) with which CD8 T cells are minimally affected. Upon structural analysis, JES6-1 was observed to block IL-2R $\beta$  (CD122) binding, but CD25 could peel off the antibody and allow IL-2 to bind heterotrimeric complexes.<sup>16</sup> A newly generated anti-hIL-2 antibody F5111 had a similar mode of action and could treat autoimmune disorders, such as type I diabetes in NOD mice, as well as experimental allergic encephalitis and xenogeneic graft-versus-host diseases.<sup>33</sup> IL-2/F5111 complex blocked the CD122 binding site with relatively weak affinity and CD25/IL-2 binding released F5111, allowing them to form IL-2/IL-2R $\alpha\beta\gamma$  tetrameric complex. Therefore, Treg-expanding clones might need to have a modest binding affinity to IL-2 to make their release easier.

The recent success of checkpoint blockers revolutionized tumor immunotherapy. However, their response rate is about 20–30%, and there is a critical need to combine other therapeutic modalities such as conventional chemo-radiotherapy, intestinal microbiome or immunological adjuvants to enhance its efficacy.<sup>34,35</sup> Of them, IL-2 is one of the best candidates to expand immune cells in the body, and we showed that a cytokine-antibody complex-based approach could maximize its efficacy while minimizing its adverse effects.

### Author contribution

J.Y.L. performed the experiments and drafted the manuscript. E.L., S.W.H, D. K. E.O., performed the experiments. S.H.I and J.S. helped experimental design. C.D.S., initiated the study but has passed away in the middle of project development. Y.J.L., designed the experiments and edited the manuscript.

### Disclosure of potential conflict of interest

J.Y.L works for Selexcine. The other authors declare no competing interests.

### Funding

This work was supported by project [IBS-R005-D1] of the Institute for Basic Science, and [NRF-2019R1F1A1059237] of Korean Ministry of Science, Information/Communication Technology and Future Planning.

**ORCID**You Jeong Lee  <http://orcid.org/0000-0002-6786-6955>**References**

- Boyman O, Sprent J. The role of interleukin-2 during homeostasis and activation of the immune system. *Nat Rev Immunol.* 2012;12(3):180–190. doi:10.1038/nri3156.
- Boyman O, Kovar M, Rubinstein MP, Surh CD, Sprent J. Selective stimulation of T cell subsets with antibody-cytokine immune complexes. *Science.* 2006;311(5769):1924–1927. doi:10.1126/science.1122927.
- Wang X, Rickert M, Garcia KC. Structure of the quaternary complex of interleukin-2 with its alpha, beta, and gamma receptors. *Science.* 2005;310(5751):1159–1163. doi:10.1126/science.1117893.
- Rickert M, Wang X, Boulanger MJ, Goriatcheva N, Garcia KC. The structure of interleukin-2 complexed with its alpha receptor. *Science.* 2005;308(5727):1477–1480. doi:10.1126/science.1109745.
- Arenas-Ramirez N, Woytschak J, Boyman O. Interleukin-2: biology, design and application. *Trends Immunol.* 2015;36(12):763–777. doi:10.1016/j.it.2015.10.003.
- Chinen T, Kannan AK, Levine AG, Fan X, Klein U, Zheng Y, Gasteiger G, Feng Y, Fontenot JD, Rudensky AY, et al. An essential role for the IL-2 receptor in Treg cell function. *Nat Immunol.* 2016;17(11):1322–1333. doi:10.1038/ni.3540.
- Rosenberg SA. IL-2: the first effective immunotherapy for human cancer. *J Immunol.* 2014;192(12):5451–5458. doi:10.4049/jimmunol.1490019.
- Krieg C, Letourneau S, Pantaleo G, Boyman O. Improved IL-2 immunotherapy by selective stimulation of IL-2 receptors on lymphocytes and endothelial cells. *Proc Natl Acad Sci U S A.* 2010;107(26):11906–11911. doi:10.1073/pnas.1002569107.
- Schwartz RN, Stover L, Dutcher J. Managing toxicities of high-dose interleukin-2. *Oncology (Williston Park).* 2002;16:11–20.
- Lotze MT, Frana LW, Sharrow SO, Robb RJ, Rosenberg SA. In vivo administration of purified human interleukin 2. I. Half-life and immunologic effects of the Jurkat cell line-derived interleukin 2. *J Immunol.* 1985;134(1):157–166.
- Arenas-Ramirez N, Zou C, Popp S, Zingg D, Brannetti B, Wirth E, Calzascia T, Kovarik J, Sommer L, Zenke G, et al. Improved cancer immunotherapy by a CD25-mimobody conferring selectivity to human interleukin-2. *Sci Transl Med.* 2016;8(367):367ra166. doi:10.1126/scitranslmed.aag3187.
- Lee YJ, Wang H, Starrett G, Phuong V, Jameson S, Hogquist K. Tissue-specific distribution of iNKT cells impacts their cytokine response. *Immunity.* 2015;43(3):566–578. doi:10.1016/j.immuni.2015.06.025.
- Yokoyama WM, Christensen M, Santos GD, Miller D. Production of monoclonal antibodies. *Curr Protoc Immunol.* 2006;Chapter 2:Unit 2.5.
- Fields C, O'Connell D, Xiao S, Lee GU, Billiald P, Muzard J. Creation of recombinant antigen-binding molecules derived from hybridomas secreting specific antibodies. *Nat Protoc.* 2013;8(6):1125–1148. doi:10.1038/nprot.2013.057.
- Castle JC, Kreiter S, Diekmann J, Lower M, van de Roemer N, de Graaf J, Selmi A, Diken M, Boegel S, Paret C, et al. Exploiting the mutanome for tumor vaccination. *Cancer Res.* 2012;72(5):1081–1091. doi:10.1158/0008-5472.CAN-11-3722.
- Spangler JB, Tomala J, Luca V, Jude K, Dong S, Ring A, Votavova P, Pepper M, Kovar M, Garcia K, et al. Antibodies to interleukin-2 elicit selective T cell subset potentiation through distinct conformational mechanisms. *Immunity.* 2015;42(5):815–825. doi:10.1016/j.immuni.2015.04.015.
- Silva D-A, Yu S, Ulge UY, Spangler JB, Jude KM, Labão-Almeida C, Ali LR, Quijano-Rubio A, Ruterbusch M, Leung J, et al. De novo design of potent and selective mimics of IL-2 and IL-15. *Nature.* 2019;565(7738):186–191. doi:10.1038/s41586-018-0830-7.
- Elpek KG, Rubinstein MP, Bellemare-Pelletier A, Goldrath AW, Turley SJ. Mature natural killer cells with phenotypic and functional alterations accumulate upon sustained stimulation with IL-15/IL-15Ralpha complexes. *Proc Natl Acad Sci U S A.* 2010;107(50):21647–21652. doi:10.1073/pnas.1012128107.
- Fogel LA, Sun MM, Geurs TL, Carayannopoulos LN, French AR. Markers of nonselective and specific NK cell activation. *J Immunol.* 2013;190(12):6269–6276. doi:10.4049/jimmunol.1202533.
- Chiossone L, Chaix J, Fuseri N, Roth C, Vivier E, Walzer T. Maturation of mouse NK cells is a 4-stage developmental program. *Blood.* 2009;113(22):5488–5496. doi:10.1182/blood-2008-10-187179.
- Liao W, Lin JX, Leonard WJ. Interleukin-2 at the crossroads of effector responses, tolerance, and immunotherapy. *Immunity.* 2013;38(1):13–25. doi:10.1016/j.immuni.2013.01.004.
- Lu YC, Robbins PF. Cancer immunotherapy targeting neoantigens. *Semin Immunol.* 2016;28(1):22–27. doi:10.1016/j.smim.2015.11.002.
- Sharpe AH. Introduction to checkpoint inhibitors and cancer immunotherapy. *Immunol Rev.* 2017;276(1):5–8. doi:10.1111/imr.2017.276.issue-1.
- Ribas A, Wolchok JD. Cancer immunotherapy using checkpoint blockade. *Science.* 2018;359(6382):1350–1355. doi:10.1126/science.aar4060.
- Lee SH, Fragoso MF, Biron CA. Cutting edge: a novel mechanism bridging innate and adaptive immunity: IL-12 induction of CD25 to form high-affinity IL-2 receptors on NK cells. *J Immunol.* 2012;189(6):2712–2716. doi:10.4049/jimmunol.1201528.
- Levin AM, Bates DL, Ring AM, Krieg C, Lin JT, Su L, Moraga I, Raeber ME, Bowman GR, Novick P, et al. Exploiting a natural conformational switch to engineer an interleukin-2 'superkine'. *Nature.* 2012;484(7395):529–533. doi:10.1038/nature10975.
- Klein C, Waldhauer I, Nicolini VG, Freimoser-Grundschober A, Nayak T, Vugts DJ, Dunn C, Bolijn M, Benz J, Stihle M, et al. Cergutuzumab amunaleukin (CEA-IL2v), a CEA-targeted IL-2 variant-based immunocytokine for combination cancer immunotherapy: overcoming limitations of aldesleukin and conventional IL-2-based immunocytokines. *Oncoimmunology.* 2017;6(3):e1277306. doi:10.1080/2162402X.2016.1277306.
- Charych DH, Hoch U, Langowski JL, Lee SR, Addepalli MK, Kirk PB, Sheng D, Liu X, Sims PW, VanderVeen LA, et al. NKTR-214, an engineered cytokine with biased IL2 receptor binding, increased tumor exposure, and marked efficacy in mouse tumor models. *Clin Cancer Res.* 2016;22(3):680–690. doi:10.1158/1078-0432.CCR-15-1631.
- Charych D, Khalili S, Dixit V, Kirk P, Chang T, Langowski J, Rubas W, Doberstein SK, Eldon M, Hoch U, et al. Modeling the receptor pharmacology, pharmacokinetics, and pharmacodynamics of NKTR-214, a kinetically-controlled interleukin-2 (IL2) receptor agonist for cancer immunotherapy. *PLoS One.* 2017;12(7):e0179431. doi:10.1371/journal.pone.0179431.
- Garber K. Cytokine resurrection: engineered IL-2 ramps up immuno-oncology responses. *Nat Biotechnol.* 2018;36(5):378–379. doi:10.1038/nbt0518-378.
- Caudana P, Núñez NG, De La Rochere P, Pinto A, Denizeau J, Alonso R, Niborski LL, Lantz O, Sedlik C, Piaggio E, et al. IL2/anti-IL2 complex combined with CTLA-4, but not PD-1, blockade rescues antitumor NK cell function by regulatory T-cell modulation. *Cancer Immunol Res.* 2019;7(3):443–457. doi:10.1158/2326-6066.CIR-18-0697.
- Hutmacher C, Gonzalo Núñez N, Liuzzi AR, Becher B, Neri D. Targeted delivery of IL2 to the tumor stroma potentiates the action of immune checkpoint inhibitors by preferential activation of NK and CD8(+) T cells. *Cancer Immunol Res.* 2019;7(4):572–583. doi:10.1158/2326-6066.CIR-18-0566.
- Trotta E, Bessette PH, Silveria SL, Ely LK, Jude KM, Le DT, Holst CR, Coyle A, Potempa M, Lanier LL, et al. A human anti-IL-2 antibody that potentiates regulatory T cells by a structure-based mechanism. *Nat Med.* 2018;24(7):1005–1014. doi:10.1038/s41591-018-0070-2.
- Zitvogel L, Ma Y, Raoult D, Kroemer G, Gajewski TF. The microbiome in cancer immunotherapy: diagnostic tools and therapeutic strategies. *Science.* 2018;359(6382):1366–1370. doi:10.1126/science.aar6918.
- Wei SC, Duffy CR, Allison JP. Fundamental mechanisms of immune checkpoint blockade therapy. *Cancer Discov.* 2018;8(9):1069–1086. doi:10.1158/2159-8290.CD-18-0367.